

# Localization and scattering of a photon in quasiperiodic qubit arrays

Xinyin Zhang ,<sup>1,2</sup> Yongguan Ke ,<sup>2,\*</sup> Zhengzhi Peng ,<sup>1,2</sup> Zuorui Chen,<sup>3</sup> Wenjie Liu ,<sup>4</sup> Li Zhang ,<sup>2</sup> and Chaohong Lee ,<sup>2,5</sup>

<sup>1</sup>*Laboratory of Quantum Engineering and Quantum Metrology, School of Physics and Astronomy, Sun Yat-Sen University (Zhuhai Campus), Zhuhai 519082, China*

<sup>2</sup>*Institute of Quantum Precision Measurement, State Key Laboratory of Radio Frequency Heterogeneous Integration, College of Physics and Optoelectronic Engineering, Shenzhen University, Shenzhen 518060, China*

<sup>3</sup>*Department of Mechanical and Aerospace Engineering, The Hong Kong University of Science and Technology, Clear Water Bay, Hong Kong, China*

<sup>4</sup>*School of General Education, Dalian University of Technology, Panjin 124221, China*

<sup>5</sup>*Quantum Science Center of Guangdong-Hong Kong-Macao Greater Bay Area (Guangdong), Shenzhen 518045, China*

(Dated: January 30, 2026)

We study the localization and scattering of a single photon in a waveguide coupled to qubit arrays with quasiperiodic spacings. As the quasiperiodic strength increases, localized subradiant states with extremely long lifetime appear around the resonant frequency and form a continuum band. In stark contrast to the fully disordered waveguide QED where all states are localized, we analytically find that the fraction of localized states is up to  $(3 - \sqrt{5})/2$  when the modulation frequency is  $(1 + \sqrt{5})/2$ . The localized and delocalized states can be related to excitation in flat and curved inverse energy bands under the approximation of large-period modulation. When the quasiperiodic strength is weak, an extended subradiant state can support the transmission of a photon. However, as the quasiperiodic strength increases, localized subradiant states can completely block the transmission of a single photon in resonance with the subradiant states, and enhance the overall reflection. At a fixed quasiperiodic strength, we also find mobility edge in transmission spectrum, below and above which the transmission is either turned on and off as system size increases. Our work give new insights into the localization in non-Hermitian systems.

## I. INTRODUCTION

Photons in a waveguide coupled to natural or artificial atoms, known as the waveguide quantum electrodynamics (WQED) system, serves as an important platform for engineering light-atom interaction and developing practical applications for quantum information processing [1–4]. WQED can be realized in a variety of experimental systems, involving cold atoms [5–7], superconducting qubits [8–10], quantum dots [11] and solid-state defects [12–14]. With current quantum technologies, it is possible to prepare and detect excitation states in atoms facilitated by a waveguide [6, 15]. Recently, many novel excitation states such as twilight states [16], bound states [17, 18], self-localized states [19], and chaos states [20, 21] have been predicted in theoretical works. It is appealing to understand the relation between excitation states and photon scattering [22]. Taking an equal-spacing qubit array as an example, subradiant states can enhance transmission [22] and inelastic scattering of photons [16].

Disorder is ubiquitous in the fabrication of WQED systems, and it can affect both photon scattering and excitation states [23–38]. Disorder at both atomic positions and transition frequencies can suppress the transmission of a single photon in a bidirectional WQED system [24, 29, 30], indicating Anderson localization. It has

been reported that all single-excitation states are localized in the thermodynamic limit of a large qubit array even with tiny randomness in positions [28]. Moreover, disorder also plays a crucial role in multi-photon scattering and photon-photon correlation. Recent research reveals that disorder in transition frequencies can induce photon antibunching through destructive interference of photon scattering paths [39]. However, the relation between localization and scattering of photons is less known in quasiperiodic structure as an intermediate phase between fully periodic and fully disordered media. Compared to disordered media, quasiperiodic media can also cause localization, but in a different and more controllable way [40], which may be more beneficial for practical applications. A question naturally arises: How do excitation states affect the scattering of a photon in a quasiperiodic WQED system?

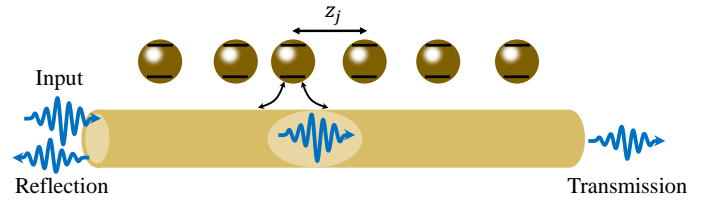


FIG. 1. Schematic diagram of a photon in a waveguide scattered by qubit arrays with quasiperiodic spacing. The positions are arranged as  $z_j = d[j + \delta \cos(2\pi\beta j + \theta)]$  with averaged spacing  $d$ , modulation strength  $\delta$ , modulation frequency  $\beta$ , and modulation phase  $\theta$ .

\* Email: keyg@szu.edu.cn

Here, we study the relation between localization of an excitation and scattering of a photon in quasiperiodic WQED, as depicted in Fig. 1. The total number of excitations and photons is conserved, and thus we can treat the scattering in the decoupled subspace with a fixed particle number. As the quasiperiodic strength increases, there appears to be a continuum band of localized excitation states near the transition frequency of the atoms. The localized states are subradiant states which have extremely long lifetimes. Unlike fully disordered case where all states are localized [28], only a fraction of excitation states are localized states. Under approximation of the large-period modulation, we find that the delocalized states and localized states come from excitation in flat inverse energy bands and curved inverse energy bands, respectively. The fraction of localized states is up to  $(3 - \sqrt{5})/2$  when the modulation frequency is  $(1 + \sqrt{5})/2$ . The subradiant extended states and localized states will support and suppress the transmission of a single photon, respectively. The overall reflection increases with the quasiperiodic strength due to the stronger localization of excitation. Surprisingly, we also find mobility edge in the transmission spectrum that separates localization phase (block of photon) and delocalization phase (transmission of photon).

## II. MODEL AND METHODS

### A. Quasiperiodic Waveguide QED

We consider the propagation of photons in a waveguide coupled to two-level atoms with quasiperiodic spacing, which is characterized by the Hamiltonian in real space that contains three parts [41],

$$H_R = H_A + H_F + H_I. \quad (1)$$

Here,  $H_A$  describes the energy of excitations,

$$H_A = \sum_j \hbar \omega_0 b_j^\dagger b_j, \quad (2)$$

where  $\omega_0$  is the uniform resonant frequency of the two levels in atoms,  $b_j^\dagger$  ( $b_j$ ) is the excitation creation (annihilation) operator on the  $j$ th atom.  $H_F$  describes the propagating photon in the waveguide along  $z$  direction with light velocity  $c$ ,

$$H_F = i\hbar c \int_{-\infty}^{+\infty} dz [a_L^\dagger(z) \frac{\partial}{\partial z} a_L(z) - a_R^\dagger(z) \frac{\partial}{\partial z} a_R(z)], \quad (3)$$

where  $a_L^\dagger(z)$  ( $a_L(z)$ ) and  $a_R^\dagger(z)$  ( $a_R(z)$ ) are the creation (annihilation) operators for a photon propagating to the left and right at position  $z$ , respectively.  $H_I$  describes the interaction between excitation and photon,

$$H_I = \sum_{j=1}^N \hbar g \int dz \delta(z - z_j) [(a_L^\dagger(z) + a_R^\dagger(z)) b_j + h.c.], \quad (4)$$

where  $g$  is the coupling strength, and the total number of atoms is  $N$ . The position of the  $j$ th atom is given by

$$z_j = d[j + \delta \cos(2\pi\beta j + \theta)], \quad (5)$$

where  $d$  is the spacing constant,  $\delta$  is the quasi-periodic strength,  $\beta$  is the modulation frequency, and  $\theta$  is the modulation phase. The qubit positions become quasiperiodic when  $\beta$  is an irrational number.

Alternatively, by making a Fourier transform,

$$\begin{aligned} a_L(z) &= \frac{1}{\sqrt{2\pi}} \int_{-\infty}^0 a(k) e^{ikz} dk, \\ a_R(z) &= \frac{1}{\sqrt{2\pi}} \int_0^{+\infty} a(k) e^{ikz} dk, \end{aligned} \quad (6)$$

we can derive the Hamiltonian in the momentum space,

$$\begin{aligned} H_M &= \int_{-\infty}^{+\infty} \hbar \omega_k a(k)^\dagger a(k) dk + \sum_j \hbar \omega_0 b_j^\dagger b_j \\ &+ \frac{\hbar g}{\sqrt{2\pi}} \sum_j \int_{-\infty}^{+\infty} (b_j^\dagger a(k) e^{ikz_j} + b_j a(k)^\dagger e^{-ikz_j}) dk. \end{aligned} \quad (7)$$

Here,  $a(k)$  is the annihilation operator for a photon with a wave vector  $k$ .  $\omega_k = c|k|$  is the frequency of a single photon with light velocity  $c$ .

### B. Transfer-matrix method in real space

We consider the scattering of a photon with momentum  $\kappa$  and frequency  $\omega_\kappa = c|\kappa|$  propagating rightward in the waveguide. The transmission and reflection of the photon are strongly modified by the interaction with a quasiperiodic qubit array. To solve the scattering problem of a single photon, we first introduce the transfer-matrix method in the real space.

We write an ansatz for a general eigenstate [42],

$$|E_k\rangle = \sum_j e_j b_j^\dagger |0\rangle + \int dz \phi_L(z) c_L^\dagger(z) |0\rangle + \int dz \phi_R(z) c_R^\dagger(z) |0\rangle. \quad (8)$$

with

$$\begin{aligned}\phi_R(z) &= \frac{e^{i\kappa z}}{\sqrt{2\pi}} [\theta(z_1 - z) + t_1^2 \theta(z - z_1) \theta(z_2 - z) + t_2^3 \theta(z - z_2) \theta(z_3 - z) + \dots + t(\kappa) \theta(z - z_N)], \\ \phi_L(z) &= \frac{e^{-i\kappa z}}{\sqrt{2\pi}} [r(\kappa) \theta(z_1 - z) + r_1^2 \theta(z - z_1) \theta(z_2 - z) + r_2^3 \theta(z - z_2) \theta(z_3 - z) + \dots + r_{N-1}^N \theta(z - z_{N-1}) \theta(z_N - z)].\end{aligned}\quad (9)$$

Here,  $\theta(z)$  is the Heaviside function.  $r_j^{j+1}$  ( $t_j^{j+1}$ ) is the amplitude of reflection (transmission) between the  $j$ th and  $(j+1)$ th atoms, while  $r(\kappa) \equiv r_0^1$  and  $t(\kappa) \equiv t_N^{N+1}$  are the amplitudes of reflection by the first atom and transmission through the last atom, respectively. This ansatz satisfies the eigenvalue equation  $H_R |E_\kappa\rangle = E_\kappa |E_\kappa\rangle$ , with  $E_\kappa = \hbar c |\kappa|$ . A relation between backward reflection and forward transmission can be obtained using the transfer-matrix method [43, 44],

$$\begin{aligned}\begin{pmatrix} t_\kappa \\ 0 \end{pmatrix} &= M_N M_{N-1} \dots M_1 \begin{pmatrix} 1 \\ r_\kappa \end{pmatrix} \\ &= \begin{pmatrix} T_{11} & T_{12} \\ T_{21} & T_{22} \end{pmatrix} \begin{pmatrix} 1 \\ r_\kappa \end{pmatrix},\end{aligned}\quad (10)$$

with the transfer matrix on the  $j$ th atom,

$$M_j = \begin{pmatrix} (f_\kappa + 1)^2 - f_\kappa^2 & 2f_\kappa e^{-i2\kappa z_j} \\ -2f_\kappa e^{2i\kappa z_j} & -f_\kappa^2 + (1 - f_\kappa)^2 \end{pmatrix}. \quad (11)$$

Here,  $f_\kappa = i\Gamma_0/[2(\omega_0 - c|\kappa|)]$ , and  $\Gamma_0 = g^2/c$  is the decay rate of a single excited qubit. Finally, the reflection and transmission are respectively given by

$$\begin{aligned}r_\kappa &= -\frac{T_{21}}{T_{22}}, \\ t_\kappa &= T_{11} - \frac{T_{12}T_{21}}{T_{22}},\end{aligned}\quad (12)$$

and they satisfy a conserved relation  $|r_\kappa|^2 + |t_\kappa|^2 = 1$ .

### C. Green function method in momentum space

We can alternatively use the Green function method to calculate the reflection and transmission. After injecting a right-propagating photon with momentum ( $\kappa > 0$ ) into the waveguide, it interacts with the emitters and is transferred into an excitation. The propagation of an excitation in the qubit array is governed by the Green function, which is determined by

$$G^{-1}(\omega) = \omega - H_{eff}, \quad (13)$$

with the effective Hamiltonian for an excitation [16, 18],

$$H_{eff} = \sum_j \omega_0 b_j^\dagger b_j - i\Gamma_0 \sum_{j,l} b_j^\dagger b_l e^{i\omega/c|z_l - z_j|}. \quad (14)$$

Here,  $\Gamma_0 = g^2/c$  is the radiative decay rate, and the phase constant is defined as  $\varphi = \omega d/c$ , depending on the frequency of input photon  $\omega = c|\kappa|$ , spacing constant  $d$  and the light velocity  $c$ . The hopping of excitation from  $z_l$  to  $z_j$  points is assisted by the photon emitted from the  $l$ th qubit and consequently reabsorbed by the  $j$ th qubit. When the spacing constant is small enough, the phase constant in the effective Hamiltonian can be replaced by  $\varphi = \omega_0 d/c$ , which is the so-called Markov approximation [16]. Based on the Green function method [43, 44], the reflection coefficient is given by

$$r_\kappa = -i\Gamma_0 \sum_{j,j'} G_{j,j'}(\omega_\kappa) e^{i\omega_\kappa/c(z_j + z_{j'})}, \quad (15)$$

and the transmission is given by

$$t_\kappa = 1 - i\Gamma_0 \sum_{j,j'} G_{j,j'}(\omega_\kappa) e^{i\omega_\kappa/c(z_{j'} - z_j)}, \quad (16)$$

and they also satisfy  $|r_\kappa|^2 + |t_\kappa|^2 = 1$ . Because the reflection can be immediately obtained once the transmission is known, we focus on the reflection of a single photon. To make it clear, we expand the Green function in terms of the eigenvalues  $\{\omega_n\}$  and eigenstates  $|\{\psi_n\}\rangle$  of the effective Hamiltonian,

$$G_{j,j'}(\omega_\kappa) = \sum_n \frac{\psi_n(j)\psi_n(j')}{\omega_\kappa - \omega_n}, \quad (17)$$

where the eigenstate  $|\psi_n\rangle$  has been normalized. By combining Eqs. (17) and (15), we can obtain the following result

$$r_\kappa = -i\Gamma_0 \sum_{j,j',n} e^{i\omega_\kappa/c(z_{j'} + z_j)} \frac{\psi_n(j)\psi_n(j')}{\omega_\kappa - \omega_n}, \quad (18)$$

When the frequency of the photon is in resonance with the energy of an excitation state [i.e.,  $\omega_\kappa = \text{Re}(\omega_n)$ ], then the denominator only takes the value of the imaginary part of the eigenvalue  $\text{Im}(\omega_n)$ . If the eigenstate  $|\psi_n\rangle$  is a subradiant state with  $\text{Im}(\omega_n) \ll \Gamma_0$ , then reflection is mainly determined by the properties of the  $n$ th eigenstate. Thus, reflection may give information about the localization property of subradiant states.

We have to emphasize that both the transfer-matrix method and Green function method give exactly the same results and have their advantages. The first method can handle much larger systems, and the second method gives

an intimate relation between the scattering and subradiant states. In the next section, we will show the reflection of a single photon and its relation to the properties of subradiant eigenstates.

### III. RESULTS

Our major goal is to explore the localization properties of an excitation and their relation to the scattering of a photon. According to our previous study [16], the incoherent scattering of photons can be enhanced via subradiant states of excitations. Before proceeding to the scattering of a single photon, we first study the localization of a single excitation in a quasiperiodic qubit array via the effective Hamiltonian. We reveal the localization of a single excitation in Sec. III A, give the fraction of localization under periodic approximation in Sec. III B, show how the localized single-excitation state affects the reflection of a single photon in Sec. III C, and finally, discuss the mobility edge in transmission spectrum of a single photon in Sec. III D.

#### A. Continuum band of Localized states

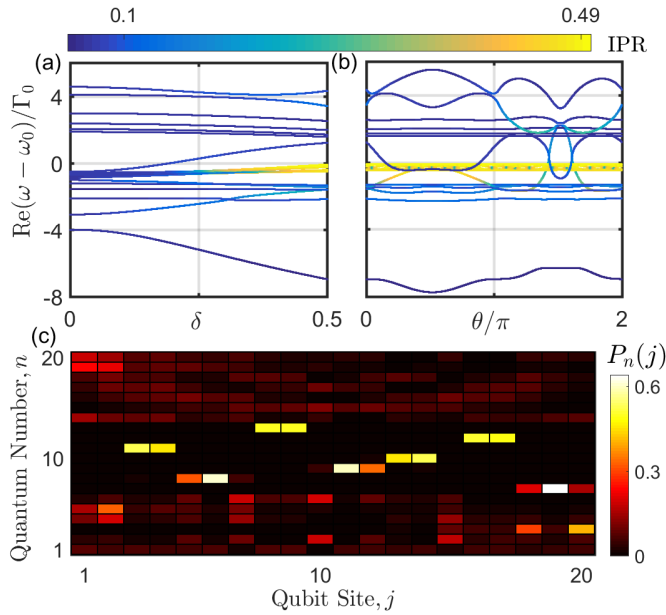


FIG. 2. Energy spectrum as a function of (a) quasiperiodic strength by fixing  $\theta = 0$  and (b) modulation phase by fixing  $\delta = 0.5$ . The colors denote the inverse participation ratio (IPR) of the corresponding eigenstates. (c) Probability distribution in the qubit array with modulation strength  $\delta = 0.5$  and modulation phase  $\theta = 0$ . The colors denote the probability  $P_n(j)$ . The other parameters are chosen as  $\omega_0 = 100$ ,  $\beta = (\sqrt{5} + 1)/2$ ,  $\Gamma_0 = 0.01$ , and  $\varphi = \omega_0 d/c = 1$ .

The eigenstates and eigenvalues are obtained by diagonalizing  $H_{\text{eff}}|\psi_n\rangle = \omega_n|\psi_n\rangle$  in the single-excitation

subspace. To characterize the localization of excitation, we calculate the inverse participation ratio (IPR)

$$\text{IPR} = \sum_j |\psi_n(j)|^4, \quad (19)$$

where  $\psi_n(j)$  is the amplitude of the excitation state at the  $j$ th site. For  $\text{IPR} \rightarrow 1$ , the excitation is completely located at a single qubit. For  $\text{IPR} \rightarrow 0$ , the excitation is completely delocalized throughout the qubit array. Thus, the larger IPR indicates that a single excitation is more localized.

We show the energy spectrum as a function of quasiperiodic strength; see Fig. 2(a). The parameters are chosen as  $\omega_0 = 100$ ,  $\beta = (\sqrt{5} + 1)/2$ ,  $\Gamma_0 = 0.01$ , and  $\varphi = \omega_0 d/c = 1$ . The colors in the spectrum indicate IPR of the corresponding eigenstates. As the quasiperiodic strength increases, some eigenstates around the resonant frequency  $\omega_0$  change from delocalization to localization. However, most of the eigenstates away from the resonant frequency still keep delocalized, except for several edge states. For a fixed large quasiperiodic strength, we can find that there exist delocalization-to-localization transitions as the energy increases. To make it clear, we calculate the energy spectrum as a function of the modulation phase; see Fig. 2(b). The other parameters are chosen the same as those in Fig. 2(a) except for  $\delta = 0.5$ . The localized states form a continuum band around the resonant frequency. As the modulation phase changes, the delocalized states may penetrate into the continuum band of localized states. However, although the penetrated delocalized states have an energy close to that of the localized states, they do not couple with the localized states. The maximum of IPR can be up to  $1/2$ , a feature value for an equal population of an excitation in two qubits. Indeed, there are several states that are mostly populated in two neighboring qubits; see the probability distribution of all the eigenstates in Fig. 2(c). The parameters are chosen the same as those in Fig. 2(a) except for  $\delta = 0.5$ . The  $y$  axis is the quantum number of eigenstates arranged in the order of incremental energy. The localized states in the continuum band are mainly located in the bulk, apart from several localized edge states.

In stark contrast to Ref. [28], in which all the eigenstates are localized in a completely disordered qubit array as the system size tends to be infinite, the localized states in the continuum band are only a fraction of the total eigenstates. In the case of  $(\sqrt{5} + 1)/2$ , the fraction of localization is up to  $(3 - \sqrt{5})/2$ .

#### B. Fraction of localization in the periodic approximation

To derive the localization fraction, we consider the periodic approximation of  $\beta = (\sqrt{5} + 1)/2$  by using a fraction representation,  $\chi/\eta = (1/1, 2/1, 3/2, 5/3, 8/5, \dots, F_{n+1}/F_n, \dots)$  with the Fibonacci sequence  $F_n$ , which satisfies  $F_n = F_{n-1} + F_{n-2}$ .

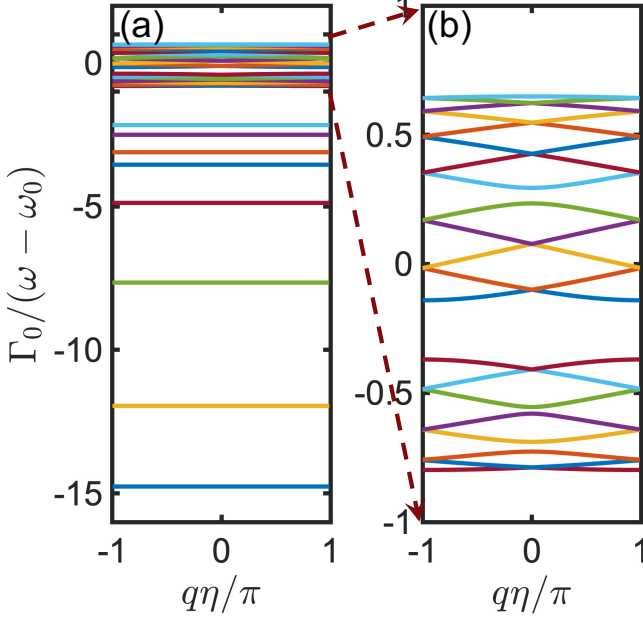


FIG. 3. (a) Inverse energy band in the large periodic approximation  $F_{n+1}/F_n = 55/34$ . (b) is the enlarged view of (a) around  $\Gamma_0 S_q \in [-1, 1]$ . The other parameters are chosen as  $\omega_0 = 100$ ,  $\Gamma_0 = 0.01$ ,  $\theta = 0$ , and  $\varphi = \omega_0 d/c = 1$ .

For the rational ratio with larger  $F_n$ , the quasiperiodic WQED makes a transition to a periodic system with translational symmetry, but still maintains some properties of the spatial modulation. In such a large-period limit, we can obtain the band structure.

According to the Bloch Theorem, the eigenstates are Bloch states.

$$|\psi_q\rangle = \sum_{j,l} e^{iq\eta j} u_l |\eta j + l\rangle, \quad (20)$$

where  $q \in [-\pi/\eta, +\pi/\eta]$  is a quasimomentum of an excitation,  $j$  is the cell index,  $l$  denotes the sublattice in a cell, and  $u_l$  are periodic functions of the Bloch states. Substituting Eq. (20) into the Schrödinger equation  $H_{eff}|\psi_q\rangle = \omega_q|\psi_q\rangle$ , the equations for  $\{u_l\}$  are given by

$$(\omega_q - \omega_0)/\Gamma_0 u_{l'} = \sum_{l=1}^{\eta} H_q(l, l') u_l, \quad (21)$$

with elements of the Bloch Hamiltonian

$$H_q(l, l') = \sin(\varphi|z_{l'} - z_l|) + \frac{i \sin(q\eta) \sin[\varphi(z_{l'} - z_l)]}{\cos(q\eta) - \cos(\varphi\eta)} + \frac{\sin(\varphi\eta) \cos[\varphi(z_{l'} - z_l)]}{\cos(q\eta) - \cos(\varphi\eta)}, \quad (22)$$

where  $H_q$  becomes a Hermitian matrix  $H_q = H_q^\dagger$ . It means that the energy band of the excitation becomes

real, because there is no way for the excitation to decay when the qubit number tends to be infinite.

To avoid the divergence of the energy band at  $q = \pm\varphi$ , we define inverse energy band as [43]

$$S_q = \frac{1}{\omega_q - \omega_0}, \quad (23)$$

which can be obtained by diagonalizing the inverse of the Bloch Hamiltonian  $H_q$ . We first calculate the inverse energy band  $S_q$  as a function of the quasi-momentum; see Fig. 3(a). The inverse energy band can be classified as flat bands in the region  $\Gamma_0|S_q| \geq 1$ , and curved bands in the region  $\Gamma_0|S_q| \leq 1$ . The flat inverse bands mean that the group velocities of these excitation states are extremely small. Even a tiny residue quasiperiodic modulation can make the slow excitation states stuck and localized. Indeed, the localized states around the resonant frequency have  $|\omega - \omega_0| \ll \Gamma_0$  and coincide with flat inverse bands. The flat inverse bands contribute to the localization of excitation. To better view the curved inverse bands, we enlarge the view around  $|\Gamma_0/(\omega - \omega_0)| \leq 1$  in Fig. 3(b). Because of the large dispersion of curved inverse bands, the group velocity of an excitation is so large that a tiny residue quasiperiodic modulation cannot localize such an excitation. Thus, the curved inverse bands contribute to the extended wave of excitation. The localization fraction is equal to the fraction of flat inverse band. The numbers of flat inverse bands and curved inverse bands are  $F_{n-2}$  and  $F_{n-1}$ , respectively. Thus, the fraction of localization is up to  $F_{n-2}/F_n = (3 - \sqrt{5})/2$  as  $F_n$  tends to be infinite.

### C. Scattering of a single photon

We are curious about how the reflection or transmission of a single photon is affected by the quasiperiodic modulation of the qubit spacings. We calculate the reflection as a function of the quasiperiodic strength and frequency of an injected photon; see Fig. 4(a) and Fig. 4(b) for its enlarged view near  $\omega_0$ . Because the subradiant states strongly affect the reflection, we also show the spectrum of subradiant states as a function of quasiperiodic strength; see the dashed blue lines. The parameters are chosen as  $\omega_0 = 100$ ,  $\Gamma_0 = 0.01$ ,  $\delta = 0.5$ ,  $\beta = (\sqrt{5} + 1)/2$ ,  $\theta = 0$ , and  $\varphi = \omega_0 d/c = 1$ . The dip of the reflection appears when the photon is in resonant with the subradiant states, except for those near resonant frequency at the large quasiperiodic strength. We find that those exceptional subradiant states are localized states which have large IPRs, as shown in Fig. 2. It seems that the delocalized (localized) subradiant states suppress (enhance) the reflection of a single photon. To estimate the effect of quasiperiodicity on reflection, we define an overall reflection as

$$\mathcal{R} = \frac{1}{\Gamma_0} \int_0^{+\infty} |r_{\omega/c}|^2 d\omega. \quad (24)$$

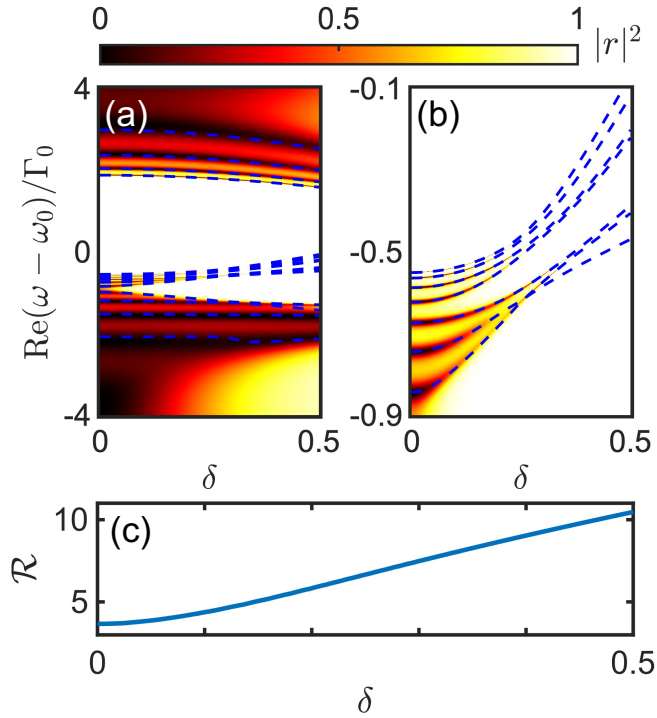


FIG. 4. (a) Reflection of a single photon as a function of quasiperiodic strength and frequency of photon, and (b) its enlarged view. (c) The overall reflection as a function of quasiperiodic strength. The parameters are chosen as  $\omega_0 = 100$ ,  $\beta = (\sqrt{5} + 1)/2$ ,  $\Gamma_0 = 0.01$ ,  $\theta = 0$ ,  $\varphi = \omega_0 d/c = 1$ .

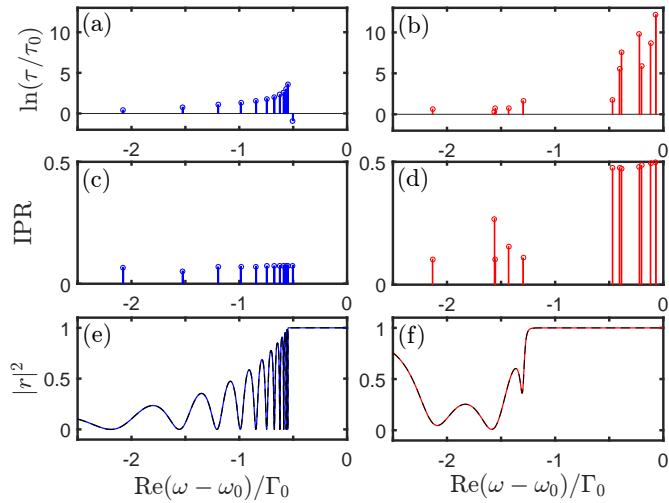


FIG. 5. Comparison between properties of excitation states and the reflection of photon. The left and right panels are the cases with no quasiperiodic modulation ( $\delta = 0$ ) and strong quasiperiodic modulation ( $\delta = 0.5$ ). (a) and (b) give the lifetime of eigenstates. (c) and (d) give the IPR of eigenstates. (e) and (f) show reflection as a function of frequency of a single photon. The blue and red solid lines are calculated via Green function method in momentum space, and the black-dashed line is calculated via transfer-matrix method in real space. The other parameters are chosen as  $\omega_0 = 100$ ,  $\Gamma_0 = 0.01$ ,  $\theta = 0$ ,  $\beta = (\sqrt{5} + 1)/2$ , and  $\varphi = \omega_0 d/c = 1$ .

where the integral is taken over the frequency of an injected photon. When  $\omega$  tends to 0 and  $+\infty$ , the reflection approach to 0. Actually, only the photon with frequency around the resonant frequency  $\omega_0$  plays a significant role. The overall reflection monotonically increases with the quasiperiodic strength; see Fig. 4(c).

To be clear, we calculate the lifetime and IPR of the excitation eigenstates, and compare them to the reflection as the frequency of photon changes; see Fig. 5. The left and right pannels are obtained without quasiperiodic modulation ( $\delta = 0$ ) and with strong quasiperiodic modulation ( $\delta = 0.5$ ), respectively. Here, we only show the results below the resonant frequency to give a better vision. The lifetime is given by  $\tau = 1/\text{Im}(\omega_n)$ , which can be used to distinguish subradiant states from superradiant states. Subradiant states have a lifetime  $\tau/\tau_0 > 1$  and superradiant states have a lifetime  $\tau/\tau_0 < 1$ , where  $\tau_0 = 1/\Gamma_0$  is the lifetime of a single excitation. In the case without quasiperiodic modulation, most of the excitation states are subradiant states below resonant frequency  $\omega_0$ , except for one superradiant state around  $\omega_0 - \Gamma_0/2$ ; see Fig. 5(a). All eigenstates are delocalized states and have small IPR; see Fig. 5(c). We find that the reflection spectrum is at a dip when the frequency of the photon is in resonance with a delocalized subradiant state; see Fig. 5(e). It means that the delocalized subradiant states suppress the reflection of the photon and reversely enhance the transmission of the photon. Moreover, the width of the dip is also related to the lifetime of the delocalized subradiant states. Generally, if the delocalized subradiant states have a longer lifetime, the resonant photon is reflected in a narrower frequency range. The photon is completely reflected when its frequency lies in the bandgap, consistent with previous results [22].

In the case with strong quasiperiodic modulation ( $\delta = 0.5$ ), the eigenstates shown in the energy window are subradiant states; see the lifetime in Fig. 5(b). The lifetime is dramatically increased for the subradiant localized states with larger IPR. This is mainly due to the fact that the localized subradiant states are strongly confined in the bulk, away from the edge qubits which are the photon leakage channel for losing excitation [45]. We find that the photon is almost perfectly reflected when its frequency is in resonance with the localized subradiant states. Similarly to the first case, there are delocalized subradiant states in the dip of the reflection spectrum. Thus, we have further confirmed that the localized (delocalized) subradiant states block (enhance) the transmission of photon.

In Figs. 5(e) and 5(f), we have to emphasize that the reflection of a single photon is calculated via the transfer-matrix method in real space (red or blue solid lines) and Green function method in momentum space (black dashed lines). The exact same results indicate that the two methods are equivalent.

#### D. Transmission mobility edge

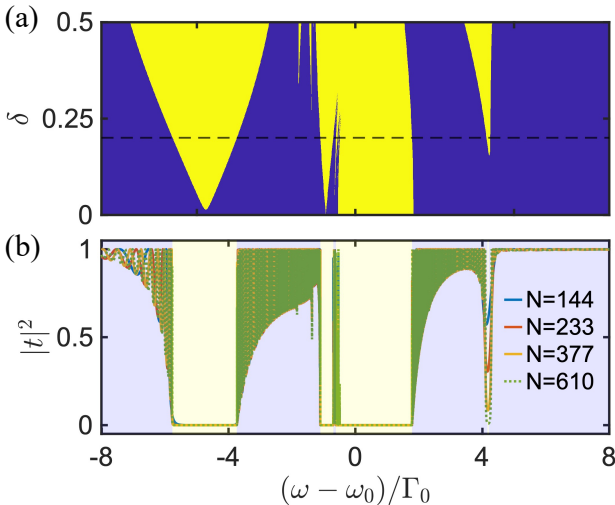


FIG. 6. (a) Localization and delocalization phases in transmission. The yellow (blue) region corresponds to the localized (delocalized) phase. Here, the transfer-matrix method is used to calculate the resistance, and the maximum number of atoms reaches  $N = 2584$ . (b) shows transmission as a function of photonic frequency for different system sizes. The blue, red, yellow solid lines and green dotted line correspond to atom numbers  $N = 144, 233, 377, 610$ , respectively. The modulation strength is fixed at  $\delta=0.2$ , corresponding to the black dashed line in panel (a). Other parameters are  $\omega_0 = 100$ ,  $\Gamma_0 = 0.01$ ,  $\theta = 0$ ,  $\beta = (\sqrt{5} + 1)/2$ , and  $\varphi = \omega_0 d/c = 1$ .

Anderson localization arises from destructive interference induced by static disorder in a system [46]. Although in one- and two-dimensional Anderson systems, all states are typically localized. But in the three-dimensional systems, there exists the mobility edge that separates localized from delocalized energy eigenstates [47]. In contrast to random disorder, quasiperiodic systems can exhibit a mobility edge even in one spatial dimension. For instance, the mobility edge emerges in generalized Aubry-André-Harper (AAH) models with on-site modulations or long-range couplings [48–51]. We also observe the mobility edge in quasiperiodic waveguide QED system, which manifests as a sharp change in transmission at the critical frequency of a single photon.

As is well known, the signature of Anderson localization is the typical resistance grows exponentially with the length of system [52, 53]. We calculate the resistance in real space using the transfer-matrix method. This allows us to identify the mobility edge, at which the excitation eigenstates undergo localization transition. The dimensionless resistance is given by the Landauer formula [54, 55]

$$\rho = \frac{1 - |t_\kappa|^2}{|t_\kappa|^2}, \quad (25)$$

where  $t_\kappa$  is the transmission coefficient. Using the property  $T_{11}T_{22} - T_{12}T_{21} = 1$  of transfer matrix, the resistance can be expressed as  $\rho = T_{12}T_{21}$ .

According to the method in Refs. [52, 53], if the system is localized, the resistance is exponential increased with the system size, otherwise it is delocalized. We calculate the resistance as a function of system size  $N$  with different quasiperiodic strength and photonic frequency. If the scaling of resistance obeys feature of localization/delocalization, we color them as yellow/blue in the parameter space, respectively. Fig. 6(a) shows a color map in the parameter space. Our numerical analysis extends to a maximum system size of  $N = 2584$ , a Fibonacci number chosen to provide an accurate rational approximation of the quasiperiodic modulation. From this phase diagram, we can find sharp change from localization phase to delocalization phase as photonic frequency varies. In analog to the conventional definition of mobility edge, we term the localization-delocalization phase boundary in photonic frequency as transmission mobility edge. The transmission mobility edge separate the localization phase that blocks transmission of photons and delocalization phase that support finite transmission of photons.

There are three major localization regions in the parameter space. The localization appears only for finite modulation strength  $\delta$ , in the left localization region around  $(\omega - \omega_0)/\Gamma_0 \sim -4.7$  and the right localization region around  $(\omega - \omega_0)/\Gamma_0 \sim 4$ . These localization can be explained by the introduction of quasiperiodic modulation. However, localization exists even in the absence of quasiperiodic modulation in the middle region around  $\omega_0$ . This can be explained by large band gap of excitation around resonant frequency. However, as quasiperiodic strength increases, there also exist localized excitation states around the band gap. Hence, we can deduce that the localization is a joint effect of band gap and localized excitation states for larger quasiperiodic strength.

To further verify the validation of mobility edge, we fix quasiperiodic strength  $\delta = 0.2$  and calculate the transmission as a function of photon frequency for different system sizes. To obtain optimal rational approximation of  $\beta = (\sqrt{5} + 1)/2$ , we set the number of atoms to a sequence of Fibonacci numbers,  $N = 144, 233, 377$ , and  $610$ . The transmission will decrease with system size in the localization phase and maintain finite values in the delocalization phase. Comparing Figs. 6 (a) and (b), one can find that in the light yellow regions, the transmission indeed decreases as  $N$  increases, corresponding to the localization region. However, in the light blue regions, the transmission oscillates around finite values as  $N$  increases, corresponding to the delocalization region. The transmission mobility edges can be exactly obtained from the analysis of finite-size scaling.

#### IV. SUMMARY AND DISCUSSION

We have studied the localization and scattering of a photon in qubit arrays with quasiperiodic modulation of spacing. We have developed transfer-matrix method in real space and Green function method in momentum space to calculate the scattering of photon, and showed that the two methods give exactly the same results. As the strength of quasiperiodic modulation increases, the subradiant states gradually change from extended states to localized states. The strong quasiperiodic modulation leads to the localization of fractional eigenstates near resonant frequency, in stark contrast to disordered WQED systems where all the eigenstates are localized in the thermodynamic limit. The localized and delocalized states are respectively from the flat inverse bands and curved inverse bands in the limit of large-period modulation. The single localized excitation blocks the transmission of a photon in resonance with the excitation, but the delocalized excitation can support the transmission. Furthermore, we also find transmission mobility edge, where delocalization-localization transition in transmission happens as photonic frequency changes.

In this work, we only consider how localized single-excitation subradiant states affect the scattering of a

single photon. When considering more photons, many-body localization of excitations is predicted in disordered WQED systems when the number of photons is less than half of the chain [28]. The many-body localization of multi-excitations may play a significant role in the inelastic scattering of multiple photons. Compared to disordered WQED systems, the quasiperiodic WQED systems may have richer novel multi-excitation states, such as products of delocalized states and localized states. It is deserved to develop a more powerful method to systematically study the role of multi-excitation localization states in inelastic scattering of multiple photons and the transmission mobility edge.

#### ACKNOWLEDGMENTS

We thank Ling Lin and Na Zhang for helpful discussions. This work is supported by the National Natural Science Foundation of China (Grants No. 12275365, 12025509, and 92476201), the National Key Research and Development Program of China (Grant No. 2022YFA1404104), the Guangdong Provincial Quantum Science Strategic Initiative (GDZX2204003, GDZX2305006 and GDZX2405002), and the Natural Science Foundation of Guangdong Province (Grant No. 2023A1515012099).

---

[1] D. Roy, C. M. Wilson, and O. Firstenberg, Colloquium: Strongly interacting photons in one-dimensional continuum, *Rev. Mod. Phys.* **89**, 021001 (2017).

[2] D. E. Chang, J. S. Douglas, A. González-Tudela, C.-L. Hung, and H. J. Kimble, Colloquium: Quantum matter built from nanoscopic lattices of atoms and photons, *Rev. Mod. Phys.* **90**, 031002 (2018).

[3] R. Gutzler, M. Garg, C. R. Ast, K. Kuhnke, and K. Kern, Light-matter interaction at atomic scales, *Nat. Rev. Phys.* **3**, 441–453 (2021).

[4] A. S. Sheremet, M. I. Petrov, I. V. Iorsh, A. V. Poshakinskiy, and A. N. Poddubny, Waveguide quantum electrodynamics: Collective radiance and photon-photon correlations, *Rev. Mod. Phys.* **95**, 015002 (2023).

[5] A. Goban, C.-L. Hung, J. D. Hood, S.-P. Yu, J. A. Muniz, O. Painter, and H. J. Kimble, Superradiance for atoms trapped along a photonic crystal waveguide, *Phys. Rev. Lett.* **115**, 063601 (2015).

[6] N. V. Corzo, J. Raskop, A. Chandra, A. S. Sheremet, B. Gouraud, and J. Laurat, Waveguide-coupled single collective excitation of atomic arrays, *Nature* **566**, 359–362 (2019).

[7] R. Pennetta, M. Blaha, A. Johnson, D. Lechner, P. Schneeweiss, J. Volz, and A. Rauschenbeutel, Collective radiative dynamics of an ensemble of cold atoms coupled to an optical waveguide, *Phys. Rev. Lett.* **128**, 073601 (2022).

[8] A. F. Van Loo, A. Fedorov, K. Lalumiere, B. C. Sanders, A. Blais, and A. Wallraff, Photon-mediated interactions between distant artificial atoms, *Science* **342**, 1494–1496 (2013).

[9] Y. Liu and A. A. Houck, Quantum electrodynamics near a photonic bandgap, *Nature Physics* **13**, 48–52 (2017).

[10] E. Kim, X. Zhang, V. S. Ferreira, J. Bunker, J. K. Iverson, A. Sipahigil, M. Bello, A. González-Tudela, M. Mirhosseini, and O. Painter, Quantum electrodynamics in a topological waveguide, *Phys. Rev. X* **11**, 011015 (2021).

[11] A. Tiranov, V. Angelopoulou, C. J. van Diepen, B. Schirinski, O. A. D. Sandberg, Y. Wang, L. Midolo, S. Scholz, A. D. Wieck, A. Ludwig, A. S. Sørensen, and P. Lodahl, Collective super- and subradiant dynamics between distant optical quantum emitters, *Science* **379**, 389–393 (2023).

[12] P. Lodahl, S. Mahmoodian, and S. Stobbe, Interfacing single photons and single quantum dots with photonic nanostructures, *Rev. Mod. Phys.* **87**, 347–400 (2015).

[13] A. P. Foster, D. Hallett, I. V. Iorsh, S. J. Sheldon, M. R. Godslan, B. Royall, E. Clarke, I. A. Shelykh, A. M. Fox, M. S. Skolnick, I. E. Itskevich, and L. R. Wilson, Tunable photon statistics exploiting the fano effect in a waveguide, *Phys. Rev. Lett.* **122**, 173603 (2019).

[14] H. Le Jeannic, T. Ramos, S. F. Simonsen, T. Pregnolato, Z. Liu, R. Schott, A. D. Wieck, A. Ludwig, N. Rotenberg, J. J. García-Ripoll, and P. Lodahl, Experimental reconstruction of the few-photon nonlinear scattering matrix from a single quantum dot in a nanophotonic waveguide, *Phys. Rev. Lett.* **126**, 023603 (2021).

[15] W. S. Leong, M. Xin, Z. Chen, S. Chai, Y. Wang, and S.-Y. Lan, Large array of schrödinger cat states facilitated

by an optical waveguide, *Nature communications* **11**, 1–7 (2020).

[16] Y. Ke, A. V. Poshakinskiy, C. Lee, Y. S. Kivshar, and A. N. Poddubny, Inelastic scattering of photon pairs in qubit arrays with subradiant states, *Phys. Rev. Lett.* **123**, 253601 (2019).

[17] Y.-X. Zhang, C. Yu, and K. Mølmer, Subradiant bound dimer excited states of emitter chains coupled to a one dimensional waveguide, *Phys. Rev. Research* **2**, 013173 (2020).

[18] Y. Ke, J. Zhong, A. V. Poshakinskiy, Y. S. Kivshar, A. N. Poddubny, and C. Lee, Radiative topological biphoton states in modulated qubit arrays, *Phys. Rev. Research* **2**, 033190 (2020).

[19] J. Zhong, N. A. Olekhno, Y. Ke, A. V. Poshakinskiy, C. Lee, Y. S. Kivshar, and A. N. Poddubny, Photon-mediated localization in two-level qubit arrays, *Phys. Rev. Lett.* **124**, 093604 (2020).

[20] A. V. Poshakinskiy, J. Zhong, Y. Ke, N. A. Olekhno, C. Lee, Y. S. Kivshar, and A. N. Poddubny, Quantum hall phases emerging from atom–photon interactions, *npj Quantum Inf.* **7**, 34 (2021).

[21] A. V. Poshakinskiy, J. Zhong, and A. N. Poddubny, Quantum chaos driven by long-range waveguide-mediated interactions, *Phys. Rev. Lett.* **126**, 203602 (2021).

[22] J. D. Brehm, A. N. Poddubny, A. Stehli, T. Wolz, H. Rotzinger, and A. V. Ustinov, Waveguide bandgap engineering with an array of superconducting qubits, *npj Quantum Mater.* **6**, 10 (2021).

[23] H. P. Lüschen, P. Bordia, S. S. Hodgman, M. Schreiber, S. Sarkar, A. J. Daley, M. H. Fischer, E. Altman, I. Bloch, and U. Schneider, Signatures of many-body localization in a controlled open quantum system, *Phys. Rev. X* **7**, 011034 (2017).

[24] I. M. Mirza, J. G. Hoskins, and J. C. Schotland, Chirality, band structure, and localization in waveguide quantum electrodynamics, *Phys. Rev. A* **96**, 053804 (2017).

[25] I. M. Mirza and J. C. Schotland, Influence of disorder on electromagnetically induced transparency in chiral waveguide quantum electrodynamics, *J. Opt. Soc. Am. B* **35**, 1149–1158 (2018).

[26] D. A. Abanin, E. Altman, I. Bloch, and M. Serbyn, Colloquium: Many-body localization, thermalization, and entanglement, *Rev. Mod. Phys.* **91**, 021001 (2019).

[27] H. H. Jen and J.-S. You, Crossover from a delocalized to localized atomic excitation in an atom–waveguide interface, *Journal of Physics B: Atomic, Molecular and Optical Physics* **54**, 105002 (2021).

[28] N. Fayard, L. Henriet, A. Asenjo-Garcia, and D. Chang, Many-body localization in waveguide quantum electrodynamics, *Physical Review Research* **3**, 033233 (2021).

[29] G.-Z. Song, J.-L. Guo, W. Nie, L.-C. Kwek, and G.-L. Long, Optical properties of a waveguide-mediated chain of randomly positioned atoms, *Opt. Express* **29**, 1903–1917 (2021).

[30] J. D. Brehm, P. Pöpperl, A. D. Mirlin, A. Shnirman, A. Stehli, H. Rotzinger, and A. V. Ustinov, Tunable anderson localization of dark states, *Phys. Rev. B* **104**, 174202 (2021).

[31] H. H. Jen, Quantum correlations of localized atomic excitations in a disordered atomic chain, *Phys. Rev. A* **105**, 023717 (2022).

[32] G. Fedorovich, D. Kornovan, A. Poddubny, and M. Petrov, Chirality-driven delocalization in disordered waveguide-coupled quantum arrays, *Phys. Rev. A* **106**, 043723 (2022).

[33] L. Ji, Y. He, Q. Cai, Z. Fang, Y. Wang, L. Qiu, L. Zhou, S. Wu, S. Grava, and D. E. Chang, Superradiant detection of microscopic optical dipolar interactions, *Phys. Rev. Lett.* **131**, 253602 (2023).

[34] N. O. Gjonbalaj, S. Ostermann, and S. F. Yelin, Modifying cooperative decay via disorder in atom arrays, *Phys. Rev. A* **109**, 013720 (2024).

[35] C.-C. Wu, K.-T. Lin, I. G. N. Y. Handayana, C.-H. Chien, S. Goswami, G.-D. Lin, Y.-C. Chen, and H. H. Jen, Atomic excitation delocalization at the clean to disordered interface in a chirally-coupled atomic array, *Phys. Rev. Res.* **6**, 013159 (2024).

[36] I. G. N. Y. Handayana, C.-C. Wu, S. Goswami, Y.-C. Chen, and H. H. Jen, Atomic excitation trapping in dissimilar chirally coupled atomic arrays, *Phys. Rev. Res.* **6**, 013320 (2024).

[37] I. G. N. Y. Handayana, Y.-L. Tsao, and H. H. Jen, Suppression of quantum correlations in a clean-disordered atom-nanophotonic interface, *Phys. Rev. Res.* **7**, 023303 (2025).

[38] S. Tirone, G. M. Andolina, G. Calajò, V. Giovannetti, and D. Rossini, Many-body enhancement of energy storage in a waveguide qed quantum battery, *Phys. Rev. A* **112**, 013717 (2025).

[39] G. Tian, L.-L. Zheng, Z.-M. Zhan, F. Nori, and X.-Y. Lü, Disorder-induced strongly correlated photons in waveguide QED, *Phys. Rev. Lett.* **135**, 153604 (2025).

[40] A. Poddubny and E. Ivchenko, Photonic quasicrystalline and aperiodic structures, *Physica E: Low-dimensional Systems and Nanostructures* **42**, 1871–1895 (2010).

[41] J.-T. Shen and S. Fan, Strongly correlated two-photon transport in a one-dimensional waveguide coupled to a two-level system, *Phys. Rev. Lett.* **98**, 153003 (2007).

[42] H. Zheng and H. U. Baranger, Persistent quantum beats and long-distance entanglement from waveguide-mediated interactions, *Phys. Rev. Lett.* **110**, 113601 (2013).

[43] Y. Ke, J. Huang, W. Liu, Y. Kivshar, and C. Lee, Topological inverse band theory in waveguide quantum electrodynamics, *Phys. Rev. Lett.* **131**, 103604 (2023).

[44] Y. Ke, Z. Peng, M. Ullah, and C. Lee, Photonic scattering in 2D waveguide QED: Quantum Goos-Hänchen shift, (2025), arXiv:2510.19230 [quant-ph].

[45] A. N. Poddubny, Quasiflat band enabling subradiant two-photon bound states, *Phys. Rev. A* **101**, 043845 (2020).

[46] P. W. Anderson, Absence of diffusion in certain random lattices, *Phys. Rev.* **109**, 1492–1505 (1958).

[47] G. Semeghini, M. Landini, P. Castilho, S. Roy, G. Spagnolli, A. Trenkwalder, M. Fattori, M. Inguscio, and G. Modugno, Measurement of the mobility edge for 3D anderson localization, *Nat. Phys.* **11**, 554–559 (2015).

[48] M. Schreiber, S. S. Hodgman, P. Bordia, H. P. Lüschen, M. H. Fischer, R. Vosk, E. Altman, U. Schneider, and I. Bloch, Observation of many-body localization of interacting fermions in a quasirandom optical lattice, *Science* **349**, 842–845 (2015).

[49] S. Ganeshan, J. H. Pixley, and S. Das Sarma, Nearest neighbor tight binding models with an exact mobility edge in one dimension, *Phys. Rev. Lett.* **114**, 146601 (2015).

[50] X. Deng, S. Ray, S. Sinha, G. V. Shlyapnikov, and L. San-

tos, One-dimensional quasicrystals with power-law hopping, *Phys. Rev. Lett.* **123**, 025301 (2019).

[51] F. A. An, K. Padavić, E. J. Meier, S. Hegde, S. Ganeshan, J. H. Pixley, S. Vishveshwara, and B. Gadway, Interactions and mobility edges: Observing the generalized aubry-andré model, *Phys. Rev. Lett.* **126**, 040603 (2021).

[52] A. D. Stone, J. D. Joannopoulos, and D. J. Chadi, Scaling studies of the resistance of the one-dimensional anderson model with general disorder, *Phys. Rev. B* **24**, 5583–5596 (1981).

[53] J. L. Pichard, The one-dimensional anderson model: scaling and resonances revisited, *Journal of Physics C: Solid State Physics* **19**, 1519 (1986).

[54] R. Landauer, Electrical resistance of disordered one-dimensional lattices, *The Philosophical Magazine: A Journal of Theoretical Experimental and Applied Physics* **21**, 863–867 (1970).

[55] D. C. Langreth and E. Abrahams, Derivation of the landauer conductance formula, *Phys. Rev. B* **24**, 2978–2984 (1981).